ACS OMEGA

http://pubs.acs.org/journal/acsodf

Article

Antibacterial and Antibiofilm Activities of Sertindole and Its Antibacterial Mechanism against *Staphylococcus aureus*

Yuanyuan Tang, Fanlu Zou, Chengchun Chen, Yiying Zhang, Zonglin Shen, Yansong Liu, Qiwen Deng,* Zhijian Yu,* and Zewen Wen*

Cite This: *ACS Omega* 2023, 8, 5415−5425

Read Online

ACCESS | Metrics & More | Article Recommendations | Supporting Information

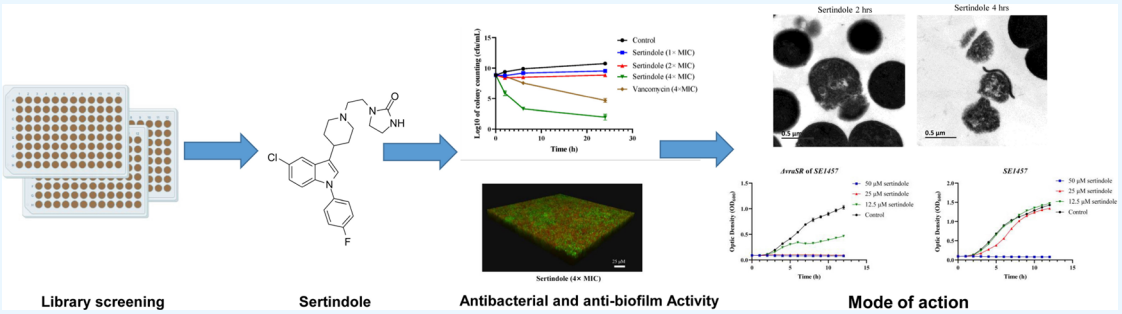

ABSTRACT: As methicillin-resistant *Staphylococcus aureus* has become the most prevalent antibiotic-resistant pathogen in many countries, there is an urgent demand to develop novel antibacterial agents. The purpose of this study is to investigate sertindole's antibacterial and antibiofilm properties, as well as its antibacterial mechanism against *S. aureus*. The MIC_{50} and MIC_{90} values for sertindole against *S. aureus* were both determined to be 50 μM, and sertindole significantly reduced *S. aureus* growth at a subinhibitory concentration of 1/2× MIC. Sertindole also showed remarkable potency in inhibiting the development of biofilms. Additionally, proteomic analysis revealed that sertindole could dramatically decrease the biosynthesis of amino acids and trigger the cell wall stress response and oxidative stress response. A series of tests, including membrane permeability assays, quantitative real-time reverse transcription-PCR, and electron microscope observations, revealed that sertindole disrupts cell integrity. The two-component system VraS/VraR knockout *S. epidermis* strain also showed enhanced sensitivity to sertindole. Overall, our data suggested that sertindole exhibited antibacterial and biofilm-inhibiting activities against *S. aureus* and that its antibacterial actions may involve the destruction of cell integrity.

INTRODUCTION

Staphylococcus aureus is a common Gram-positive bacterium that causes both community and hospital-acquired infections.[1] Infections by *S. aureus* have the potential to lead to pneumonia, endocarditis, osteomyelitis, and sepsis, and serious infections can even lead to death.[2] This is because *S. aureus* possesses a number of virulence factors that can contribute to the pathogenicity. Additionally, *S. aureus* rapidly acquires antibiotic resistance due to gene mutation and horizontal gene transfer.[3] With the appearance and rise of methicillin-resistant *S. aureus* (MRSA) compared with infections caused by methicillin-sensitive *S. aureus* (MSSA), MRSA infection was associated with enhanced length of hospital stay, morbidity, and mortality.[4,5] MRSA continues to have the greatest fatality rate among antibiotic-resistant infections in the United States. The Centers for Disease Control reported that MRSA infections resulted in about 20,000 mortality in 2018.[6] Actually, one of the most essential ways for *S. aureus* to maintain infection is by forming biofilms. Communities of microorganisms called biofilms adhere to the extracellular matrix released by bacterial cells.[7] Biofilm formation is directly linked to about 80% of bacterial infections.[8] The formation of biofilms by *S. aureus* resulted in reduced antibiotic susceptibility and evasion of phagocytosis from host immune cells. When the concentration of antibiotics decreases, bacterium will rapidly proliferate to fill the biofilm and shed into the surrounding tissues and blood, inducing recurrence, leading to chronic infection and prolonged treatment.[9] Because of the poor clinical outcomes of *S. aureus* infections, the development of novel antibacterial drugs that may both suppress planktonic cell growth and biofilm formation has become a subject of attention in recent years.[10]

Received: October 12, 2022
Accepted: January 25, 2023
Published: February 3, 2023

The development of new drugs is a time-consuming and expensive procedure that always results in a high failure rate due to safety and toxicity issues. The identification of the antibacterial activity of currently approved clinical drugs (drug repurposing) has emerged as an acceptable strategy of exploring new antibacterial therapeutics in consideration of the challenges in developing new antibacterial drugs. It is emphasized that drugs identified using this strategy have substantial toxicological and pharmacological information, which minimizes the cost and time it takes to develop new drugs.[11,12]

During the screening of Food and Drug Administration (FDA)-approved clinical compounds with antibacterial action, we noticed that sertindole (Figure 1), an atypical antipsychotic drug,[13] can suppress the growth of *S. aureus* planktonic cells. Although the antibacterial activity of some analogues or antipsychotics has been reported,[14] sertindole's antimicrobial effect has not yet been described, yet. Here, we systematically assessed sertindole's antibacterial and antibiofilm activity against *S. aureus*, and we also sought into its mode of action (MoA) using quantitative proteomics, quantitative real-time reverse transcription-PCR (qRT-PCR), transmission electron microscopy, and the susceptibility of the two-component system VraS/VraR knockout strain (VraSR). Our research suggests that sertindole possesses significant antimicrobial activity and could serve as a promising primary structure for pharmacological optimization for the treatment of multidrug-resistant bacteria.

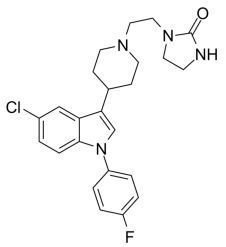

Figure 1. Chemical structure of sertindole. CAS No.: 106516-24-9.

RESULTS

In Vitro Antimicrobial Activity of Sertindole against *S. aureus*. The minimal inhibitory concentration (MIC) values of sertindole against 20 clinical isolates of *S. aureus* were determined by broth microdilution. The results indicated that the MIC values of sertindole against clinical and standard *S. aureus* strains were mainly distributed from 25 (≈11 μg/mL) to 50 μM (≈22 μg/mL), including linezolid-intermediates and MRSA isolates (Table 1). In addition, the growth curve analysis showed that sertindole could significantly inhibit the growth of *S. aureus* planktonic cells without affecting the maximum growth level at 1/2× MIC, while the growth of planktonic bacteria was completely inhibited at 1× MIC (Figure 2). These results showed that sertindole had the potential as an antibacterial drug against *S. aureus*. MICs of sertindole against clinical *S. epidermidis*, *Enterococcus faecalis*, *Enterococcus faecium*, *Klebsiella pneumoniae*, *Escherichia coli*, and *Pseudomonas aeruginosa* were also measured. As shown in Supplementary Table S1, sertindole showed broad-spectrum antibacterial activity against Gram-positive bacteria. However, no inhibitory activity was observed against Gram-negative

Table 1. Antimicrobial Susceptibility of *S. aureus* to Sertindole and Common Clinical Antibiotics[a]

	MIC (mg/L)								MIC (μM)
stains	Oxa	Cef	Van	LZD	Dap	Azi	Cli	Fos	sertindole
					MSSA				
CHS101	0.5	0.5	1	2	2	1	0.25	2	50
YUSA21	0.5	1	1	4	2	1	0.25	8	50
YUSA152	0.5	0.5	1	2	2	1	0.25	4	50
YUSA154	0.5	0.5	1	2	4	1	0.25	2	25
YUSA157	0.25	0.25	2	2	4	1	0.5	4	50
YUSA212	0.5	1	1	1	2	1	0.25	2	25
SE13	0.25	0.5	0.5	2	2	1	0.25	2	50
SE16	0.5	1	1	2	2	1	0.25	2	50
YUSA61	0.5	1	1	4	2	>256	0.25	2	25
YUSA80	0.5	1	1	4	2	1	0.25	2	50
SA113	0.25	0.25	1	2	2	32	0.0625	2	50
					MRSA				
CHS350	>512	>512	2	2	2	>256	0.5	>512	50
CHS712	>512	>64	1	4	2	>256	>2	>512	50
CHS736	>512	>512	2	4	4	>256	>2	>512	50
CHS780	>512	>64	1	4	4	>256	>2	>512	25
YUSA139	>64	>64	1	4	4	>256	0.5	>512	50
YUSA142	>64	>64	1	4	4	>256	0.5	>512	50
YUSA145	>64	>64	1	4	4	>256	0.5	>512	50
USA300	32	4	0.5	2	2	128	0.0625	4	50
HaMRSA118	16	>64	1	4	4	>256	>32	2	50
HaMRSA129	>64	>64	1	4	4	>256	>32	>512	25
HaMRSA19	>64	>64	1	4	4	>256	>32	>512	50

[a]MIC, Minimum inhibitory concentration; Oxa, Oxacillin; Cef, Cefazolin; Van, Vancomycin; LZD, Linezolid; Dap, Daptomycin; Azi, Azithromycin; Cli, Clindamycin; Fos, Fosfomycin; MSSA, methicillin-sensitive *S. aureus*; MRSA, methicillin-resistant *S. aureus*.

https://doi.org/10.1021/acsomega.2c06569
ACS Omega 2023, 8, 5415−5425

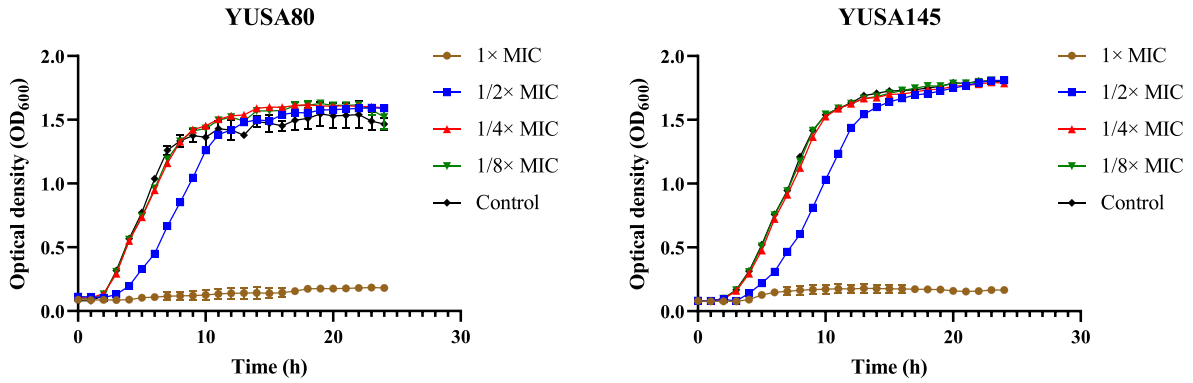

Figure 2. Effects of different concentrations of sertindole on the growth curves of clinical MSSA (*YUSA80*) and MRSA (*YUSA145*). MICs of all the isolates used in the experiment were 50 μM, and sertindole concentrations (1/8×, 1/4× ,1/2×, and 1× MIC) were tested. Absorbance at 600 nm wavelength (OD_{600}) was measured at intervals of 1 h for 24 h. Data are presented as means ± SD.

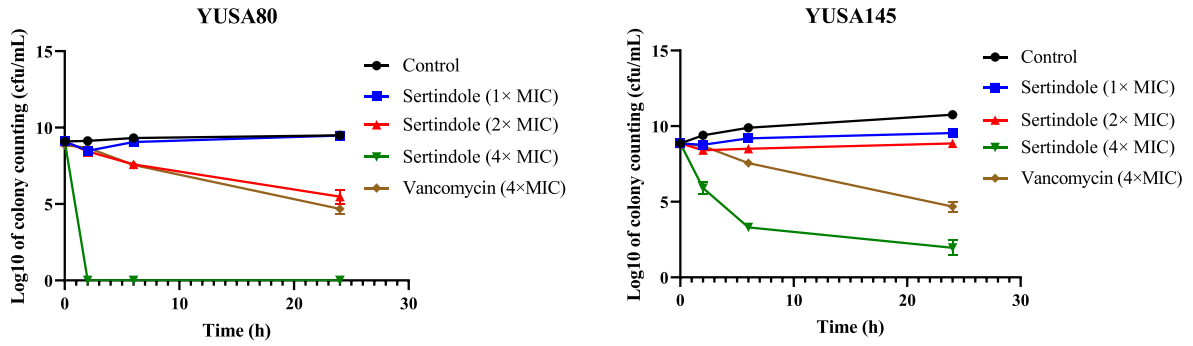

Figure 3. Time-kill assay of sertindole against clinical MSSA (*YUSA80*) and MRSA (*YUSA145*). The planktonic cells of clinical *S. aureus* isolates were treated with 1×, 2×, and 4× MIC of sertindole or 0.1% DMSO (control). Samples were harvested and counted at 0, 2, 6, and 24 h, the experiments were conducted in triplicate and presented as mean ± SD.

bacteria. In addition, the potential antibacterial activity of nine other FDA-approved indoles was evaluated, and it was found that only umifenovir showed a weak antibacterial effect against *S. aureus* (Supplementary Table S2).

In order to evaluate the bacterial killing effect of sertindole on *S. aureus*, the time killing studies were carried out. As shown in Figure 3, sertindole can completely inhibit the growth of *S. aureus* at 1× MIC while a slightly bactericidal effect was observed at 2× MIC. However, while at 4× MIC, sertindole displayed a strong bactericidal effect on both clinical MRSA and MSSA isolates, especially for MSSA, the CFUs decreased to lower than the limit of detection within 2 h, which was significantly stronger than 4× MIC of vancomycin.

Antibiofilm Activity of Sertindole. Quantitative assay of biofilm formation with crystal violet staining suggested that sertindole with a concentration of 1/4× MIC can cause a significant decrease of the biofilm formation of tested *S. aureus* isolates, whether MSSA or MRSA (Figure 4A and Supplementary Figure S1). Moreover, sertindole decreased at least 80% biofilm formation of all MSSA isolates tested at the concentration of 1/2× MIC, which indicated that sertindole significantly inhibited the biofilm formation of *S. aureus*, and the inhibitory effect on MSSA was stronger than that on MRSA. Consistent with the crystal violet staining results, a noticeable biofilm inhibition by 1/4× MIC sertindole was observed in the confocal microscopy images (Figure 4B). The effect of sertindole on mature biofilms was further assessed by confocal laser scanning microscopy (CLSM) using live/dead staining. SYTO9 and propidium iodide (PI) could dye living cells and dead cells to green and red, respectively. The results showed that a concentration of 4× MIC could markedly reduce the count of the live bacteria cells and markedly increase the percentages of dead bacteria cells (stained red) in comparison to the control (Figure 4C), suggesting the capability of sertindole for killing the bacteria cells embedded in biofilms. Consistent with that, although sertindole did not reduce the preformed biofilms of *S. aureus*, 4× MIC sertindole challenge resulted in a >2 log decrease in CFU compared to the untreated control (Supplementary Figure S2).

Proteomic Response of *S. aureus* to Sertindole. Quantitative label-free proteomic analysis was performed to understand the impact of sertindole on the *S. aureus*. The proteomic response of *S. aureus* treated with 1/2× MIC sertindole or DMSO alone was analyzed by mass spectrometry. Overall, 1293 proteins were confidently identified (matched peptides ≥1, and FDR <0.01) were confidently identified. Among the 1293 proteins quantified, 87 proteins showed significantly different expression levels (≥|1.5|-fold change, $P \leq 0.05$) compared with that in the control, containing 52 upregulated and 35 downregulated proteins in sertindole treatment (Figure 5A). Gene ontology (GO) annotations of the differential proteins according to biological processes, molecular functions, and cellular components were done using the omicsbean online database (Figure 5B). Kyoto Encyclopedia of Genes and Genomes (KEGG) analyses were performed by Database for Annotation, Visualization, and Integrated Discovery (DAVID) database. KEGG analysis revealed that the differential proteins were mainly enriched in cysteine and methionine metabolism, phosphotransferase

https://doi.org/10.1021/acsomega.2c06569
ACS Omega 2023, 8, 5415−5425

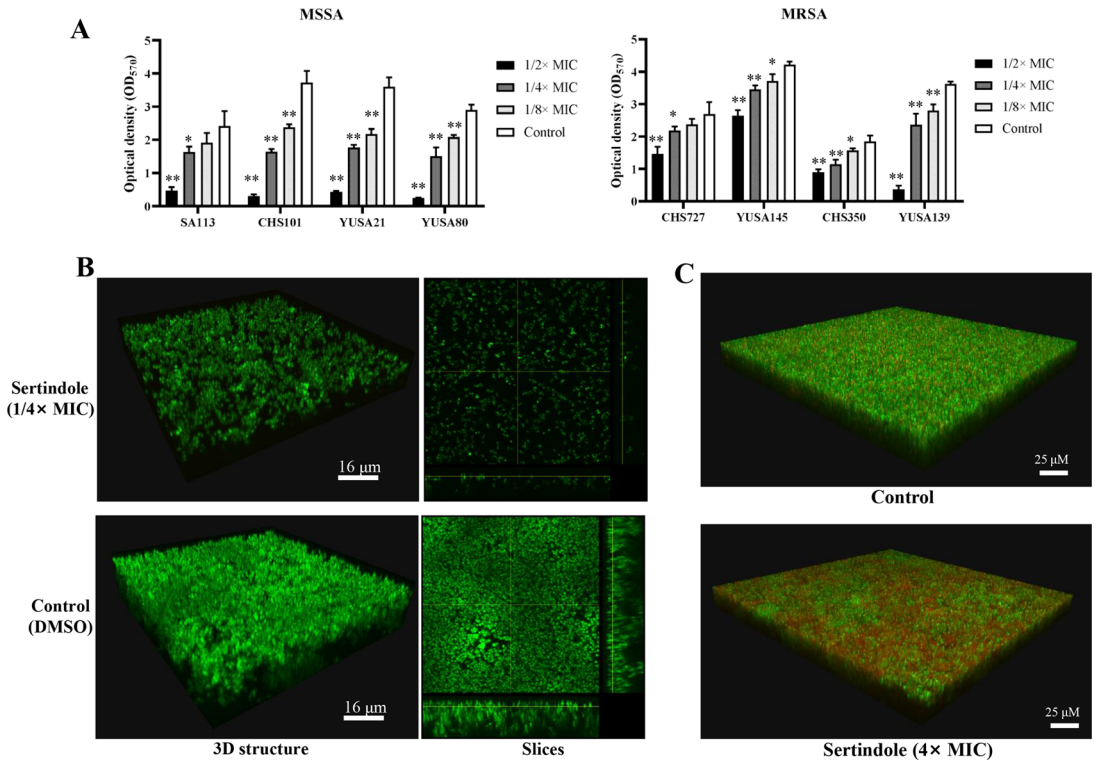

Figure 4. Antibiofilm activity of sertindole against *S. aureus*. (A) Effect of sub-inhibitory concentrations (1/8×, 1/4×, and 1/2× MIC) on the biofilm formation of eight clinical *S. aureus* isolates (including four MSSA and four MRSA). Data were represented by mean ± SD. $^{*}P < 0.05$, $^{**}P < 0.01$, Student's *t* test. (B) Effect of sertindole on the biofilm formation of the *S. aureus* observed by CLSM. 1/4× MIC (12.5 μM) sertindole was added to *S. aureus* cultures at $t = 0$. The 24 h biofilms grown on a cover glass in a cell culture dish were visualized using live/dead viability staining under a CLSM. (C) Impact of 4× MIC sertindole against the viable cells embedded in mature biofilms of *S. aureus*. Bacterial cells were inoculated onto a cell-culture dish for 24 h at 37 °C until mature biofilms were formed. After being treated with sertindole under the concentration of 4× MIC or solvent control for another 24 h, the viability of the viable or dead cells embedded in the mature biofilm was observed by confocal microscopy using live/dead staining.

system, amino acid sugar and nucleotide sugar metabolism, amino acid biosynthesis, and *S. aureus* infection (Figure 5C).

Protein−protein interaction (PPI) network analysis was constructed using the STRING database. The results showed that the downregulated proteins were enriched in enzymes related to amino acid metabolism, including aspartate kinase, glycine dehydrogenase, serine dehydrogenase, threonine synthase, methionine synthase metE and transferase metN2, cell surface-related proteins such as agglutination factor A, amidophosphoribosyltransferase purF, immunoglobulin binding protein sbi, cell surface related calcium binding protein sdrD, and ribosomal component proteins such as rpmJ, rplO, and hpf (Figure 6A). In addition, the upregulated proteins were enriched in the two-component regulatory system VraS/VraR, lipoteichoic acid (LTA) biosynthesis-related enzymes dltA and fmtA, ribosome maintenance-related proteins such as ribosome maturation factor rimP and ribosomal turnover protein frr, and phosphotransferase system enzymes and related proteins, as well as bacterial oxidative stress system-related proteins such as trxA, tpx, nfrA, msrB, and ABD29960 (Figure 6B).

Antibacterial Mechanism of Sertindole against *S. aureus*. It is noteworthy that the expression of LTA biosynthetic enzymes dltA and fmtA and phosphatidylglycerol lysyltransferase mprF was upregulated after sertindole treatment. LTA plays major roles in bacterial growth, cell wall physiology, membrane homeostasis, and virulence.[16] In addition, the expression of two-component system VraS/VraR, which was the vital regulatory system of *S. aureus* response to cell wall and membrane stress, was both upregulated. To verify whether VraS/VraR expression responds to Sertindole, the transcription of VraS/VraR treated with sertindole was investigated by qRT-PCR. Both *VraS* expression and *VraR* expression were upregulated (7.2-fold and 7.3-fold increases, respectively) under the stress of 1/2× MIC sertindole, indicating that sertindole may exert antibacterial activity by destroying cell integrity (Figure 7A). Accordingly, we evaluated the impact of sertindole on the membrane permeability of *S. aureus* using SYTOX green. Increased cell membrane permeability was observed after sertindole exposure (Figure 7B). A similar phenomenon was observed using the membrane potential sensitive dye DiBAC4(3) (Supplementary Figure S3), suggesting that sertindole could depolarize the membrane potential. To visually observe cell integrity disruption by sertindole, transmission electron microscopy (TEM) was employed. As shown in Figure 7C, the TEM showed that the boundary of the cell membrane became blurred and undermined after treatment, and intracellular contents were observed to leak from the planktonic cells. In contrast, the cell membrane of the control group was unaffected. After treatment with sertindole for 4 h, it was observed that the bacterial cytoplasm in some planktonic cells had completely bareness and some cell wall fragments could be seen. Therefore, these results further demonstrated that sertindole destroyed cell integrity of *S. aureus*.

https://doi.org/10.1021/acsomega.2c06569
ACS Omega 2023, 8, 5415−5425

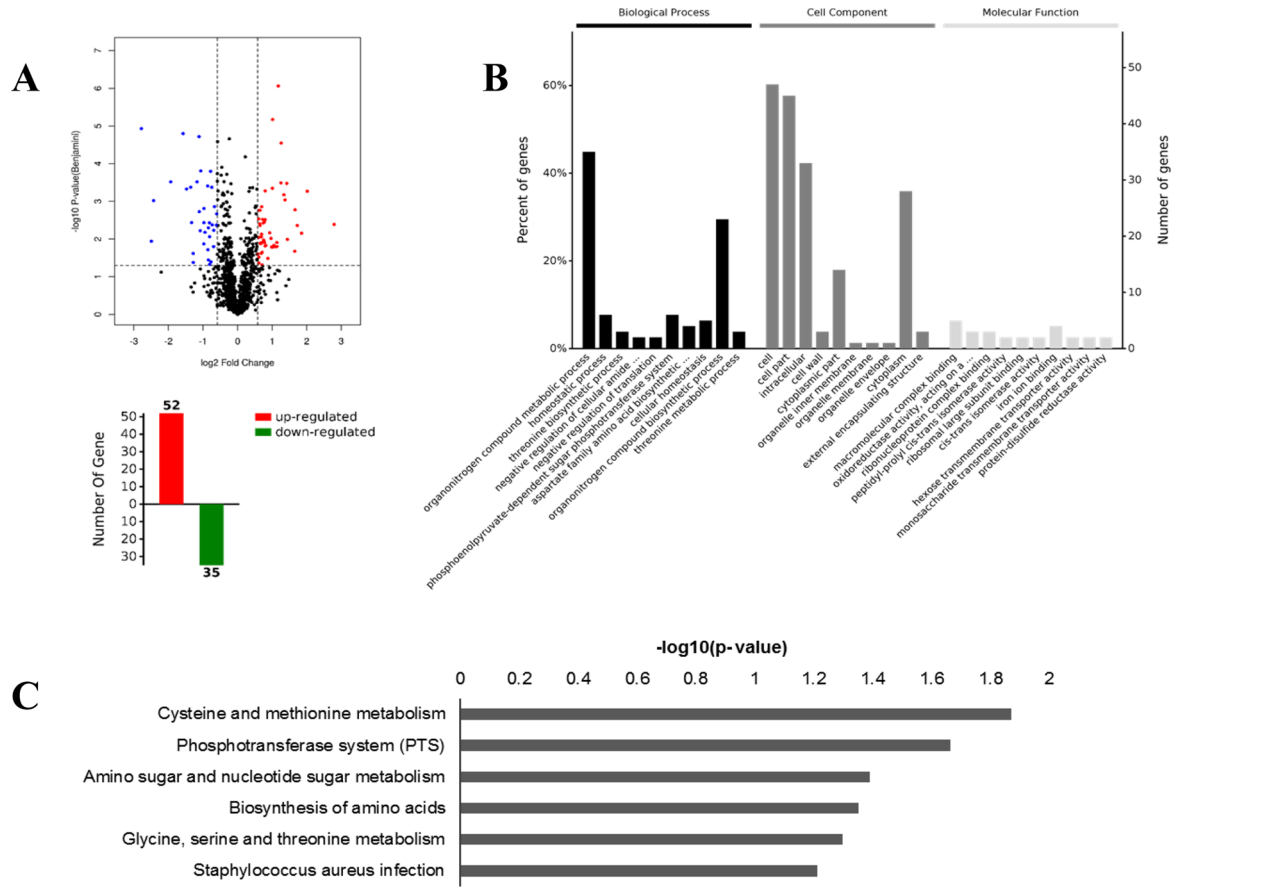

Figure 5. Differentially expressed proteins between the control groups and sertindole-treated groups found by LC−MS. (A) Volcano map and total number of differentially expressed proteins, the horizontal axis represents the ratio of differentially expressed proteins in the sertindole-treated group and untreated group of *S. aureus*, the red point shows upregulated proteins, and blue shows downregulated proteins. The vertical axis represents the *P*-value between the two groups. (B) GO analysis applied to differentially expressed proteins according to biological process. (C) KEGG analysis of the differentially expressed proteins using the DAVID database.[15]

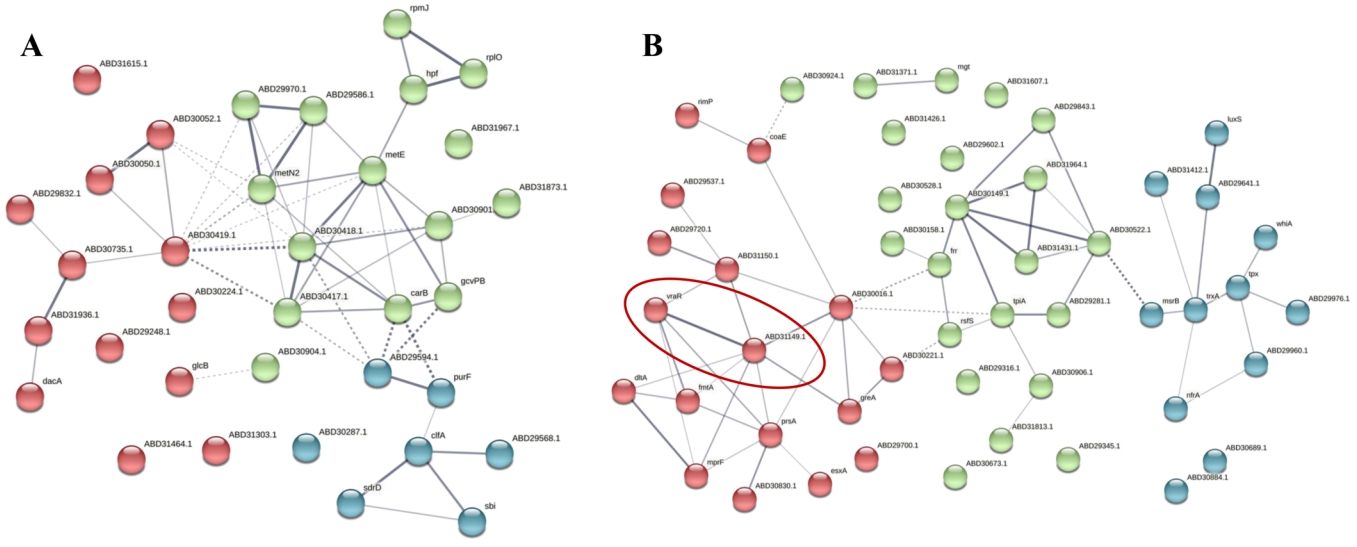

Figure 6. PPI network analysis for downregulated proteins (A) and upregulated proteins (B) after treated with 1/2× MIC sertindole based on the STING database. Line thickness indicates the strength of data support. VraS and VraR are labeled by a red ellipse.

S. epidermidis is the most prevalent species of coagulase-negative staphylococci (CoNS) involved in human infections, which is closely related but has less pathogenicity than *S. aureus*.[17,18] It has been suggested that *S. epidermidis* could exchange DNA with *S. aureus* via typical *S. aureus* phages, and the acquisition of molecular determinants of methicillin resistance, virulence, and colonization factors alter the lifestyle of *S. epidermidis* from a commensal to pathogen.[19] The two-

https://doi.org/10.1021/acsomega.2c06569
ACS Omega 2023, 8, 5415−5425

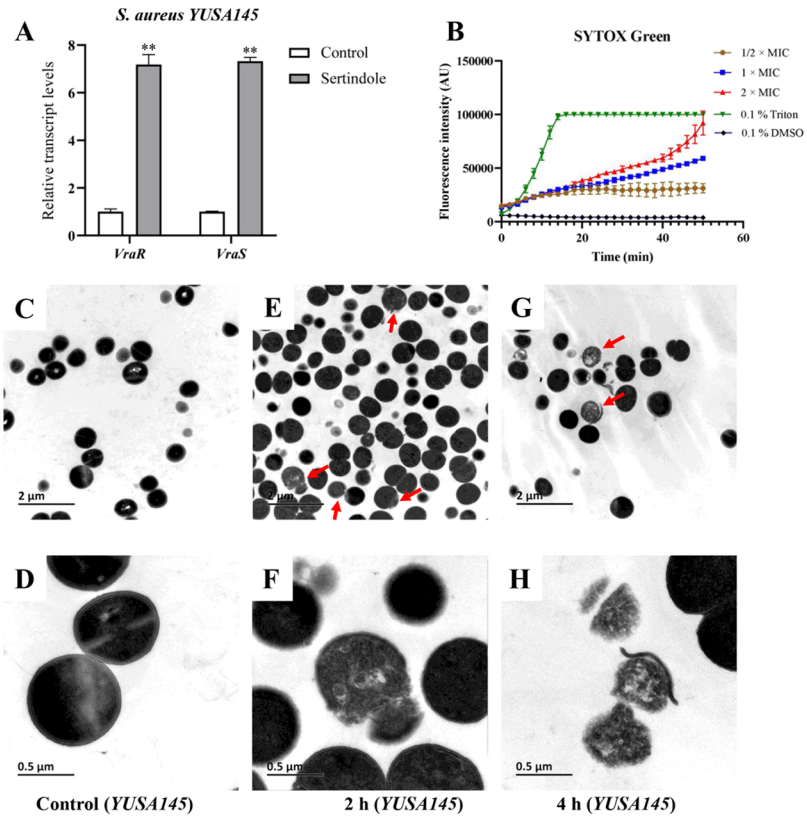

Figure 7. Mechanism of the antibacterial effect of sertindole against *S. aureus*. (A) Transcriptional levels of *vraS* and *vraR* in *S. aureus YUSA145* under sertindole stress. *YUSA145* at the logarithmic phase was treated with 1/2× MIC sertindole for 2 h of incubation. The relative expression levels of *vraS* and *vraR* were analyzed by qRT-PCR. The expression of housekeeping gene *gyrB* was used as the internal control. Data are represented as means ± SD. $^{**}P < 0.01$ (two-tailed Student's *t* test). (B) *S. aureus YUSA145* treated with various concentrations of sertindole, and the fluorescence intensity of SYTOX Green was measured by a microplate reader. (C−H) TEM images of *S. aureus YUSA145* treated with 2× MIC sertindole for 2 (E and F) and 4 h (G and H) compared with control cells (C and D). Red arrows represent areas with significant morphological changes.

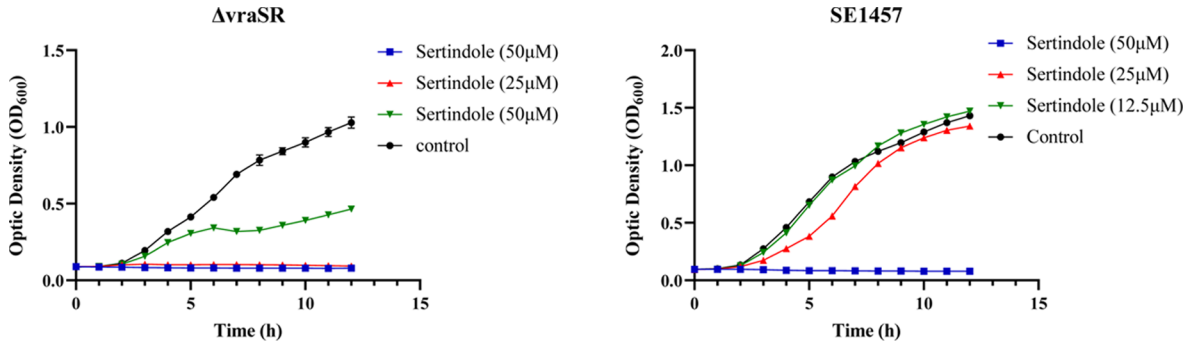

Figure 8. Growth curves of *S. epidermidis 1457* (*SE1457*) and VraS/VraR deletion mutant (Δ*vraSR*) with sertindole. The planktonic growth of *S. epidermidis* Δ*vraSR* (A) and the parent strain *SE1457* (B) was monitored under various concentrations of sertindole, including 12.5, 25, and 50 μM. Data are presented as means ± SD.

component system VraS/VraR shows a high phylogenetically conservation in *S. epidermidis* and *S. aureus* (Supplementary Figure S4). The gene sequence identity of *VraS* and *VraR* between *S. epidermidis* and *S. aureus* was 82.06 and 82.04%, respectively. The proteins share 95.22 and 91.95% sequence identity, respectively. In addition, the involvement of the two-component system VraS/VraR in the regulation of antibiotic resistance against cell wall and membrane-active antibiotics was well studied both in *S. aureus* and *S. epidermidis*.[20] We first tested whether the expression of the two-component system VraS/VraR of *S. epidermidis* was response to sertindole. The qRT-PCR results showed that the transcriptional level of *VraS* and *VraR* was upregulated by 1/2× sertindole (Supplementary Figure S5), which was in line with in the *S. aureus*. To further validate the antibacterial mechanism of sertindole, the susceptibility of VraS/VraR deletion strain (Δ*vraSR*) of *S. epidermidis* to sertindole was examined by growth curve assay.[20] As shown in Figure 8, compared with parent strain *S. epidermidis 1457* (*SE1457*), Δ*vraSR* was completely inhibited from growing at the concentration of 25 μM sertindole. In addition, the growth of Δ*vraSR* was remarkably impaired after exposed to 12.5 μM sertindole while it was unaffected in

https://doi.org/10.1021/acsomega.2c06569
ACS Omega 2023, 8, 5415−5425

wildtype. In addition, the maximum growth level of Δ*vraSR* was also smaller than that of the wildtype *SE1457* after cultured for 24 h, demonstrating that the antibacterial activity of sertindole was associated with the cell wall and membrane stress.

DISCUSSION

The emergence of drug-resistant *S. aureus* strains has led to the failure of traditional antibiotic therapy frequently, posing a serious challenge to the clinical treatment of *S. aureus* infections. Consequently, there is an urgent need to explore agents with novel antibacterial mechanisms that could overcome the barrier of antibiotic resistance. Since skipping many pharmacological optimization procedures, drug repurposing has become an attractive strategy for the development of new antibacterial drugs.[21] In order to obtain new drugs against *S. aureus*, an FDA-approved drug library was sifted, and the antibacterial activity sertindole was discovered. Sertindole is a nonsedating atypical antipsychotic with high selectivity for the mesolimbic dopaminergic pathway receptors 5-HT2A, 5-HT2C, D2, and αl[22,23] and has recently been reported to exhibit antiviral activity against Ebola virus.[24] In addition, Sertindole can induce autophagy and apoptosis of neuroblastoma cells by generating reactive oxygen species (ROS).[25] It was also reported to participate in breast cancer cell apoptosis through directly binding and inhibiting 5-HT6,[26] suggesting that sertindole has a variety of biological activities. Our results showed that sertindole could present antimicrobial activity against clinical *S. aureus* isolates with MIC_{50} and MIC_{90} of 50 μM. In addition, sertindole showed inhibition ability against clinically resistant bacteria such as MRSA and linezolid-mediated *S. aureus* isolates. Furthermore, the formation of *S. aureus* biofilms is an important virulence factor leading to chronic infections,[27] and only a few conventional antibiotics are effective against biofilms of *S. aureus* according to previous studies. Sertindole showed strong inhibition ability to *S. aureus* biofilm formation and more importantly, sertindole could penetrate mature biofilms and kill *S. aureus* cells within the biofilm matrix, suggesting the potential application of sertindole in clinical anti-infective treatment of *S. aureus*.

Elucidating the mechanism of antimicrobial compounds could both facilitate the modification of superior derivatives with improved efficacy and provide new targets for the development of novel antimicrobial compounds. Thus, we investigated the antibacterial mechanism of sertindole using proteomic techniques. The results proved that sertindole affected several metabolic pathways of *S. aureus* such as the downregulation of several amino acid biosynthesis as well as ribosomal proteins rpmJ, rplO, and hpf, indicating that partial protein synthesis in *S. aureus* was inhibited by sertindole treatment. Additionally, ribosomal maturation factor rimP and ribosomal turnover protein frr were upregulated, indicating that *S. aureus* may respond to the blocked protein synthesis by accelerating the renewal and turnover of ribosomes to ensure the biosynthesis of essential proteins for survival. In order to survive in a peroxidative environment, organisms synthesize a variety of natural antioxidants such as vitamin C, glutathione (GSH), and carotenoids. Sertindole treatment resulted in the upregulation of a large number of proteins related to the peroxidative stress system, for instance, thioredoxin, a regulator of cellular redox homeostasis whose role is to maintain a certain level of ROS in cells. Its upregulation implied that sertindole could induce excessive production of ROS, which places the bacteria under peroxidative stress. In addition, some studies have shown that ROS production might explain the antibacterial activity of antibiotics.[28]

It is noteworthy that the expression of the two-component system VraS/VraR and LTA biosynthesis-related enzymes was upregulated, wherein the phosphatidylglycerol lysyltransferase mprF has been reported to be involved in the emerging of daptomycin and vancomycin resistance.[29−33] The mode of action of daptomycin is disrupting the functional integrity of the bacterial membrane while that of vancomycin is inhibiting cell wall synthesis. Likewise, the two-component system VraS/VraR regulates cell wall biosynthesis, and both *S. aureus* and *S. epidermidis* could rapidly respond to antibiotics targeting cell wall biosynthesis peptidoglycan like β-lactams and vancomycin.[34] Multiple single nucleotide polymorphism locus within *VraS/VraR* could be detected in vancomycin-intermediary *S. aureus* (VISA) strains,[35] and deletion of the *vraS* or *vraR* genes had been shown to resensitize *S. aureus* to β-lactams and vancomycin.[36] More importantly, VraS/VraR has been reported contributing to lower mprF-mediated susceptibility of daptomycin. In this study, the destruction of cell integrity of *S. aureus* by sertindole was proved by increased SYTOX Green and depolarization of membrane potential by DiBAC4(3) fluorescence and damaged cell walls observed by TEM. In addition, the transcription of *VraS* and *VraR* in both *S. aureus* and *S. epidermidis* can be facilitated by sertindole. Moreover, the Δ*vraSR* strain, with a disrupted and thinner cell wall,[20] displayed enhanced susceptibility to sertindole. To sum up, these data indicated that destruction of *S. aureus* cell integrity was related to the potential antibacterial mechanism of sertindole.

CONCLUSIONS

In conclusion, we first described the antibacterial and biofilm-inhibiting capabilities of sertindole against *S. aureus*, and the antibacterial mechanism of sertindole was mainly due to the disruption of bacterial cell integrity. The MIC of sertindole is still higher compared to first-line clinical antibiotics, which limits its clinical application and could only make it be used as a topical antimicrobial agent. However, further modification of the molecular structure of sertindole to obtain derivatives with better antibacterial activity requires the identification of key pharmacodynamic groups. Therefore, further identification of direct targets of sertindole's antibacterial activity is of vital importance in promoting the development of sertindole's application, with the goal to provide new options against serious infections caused by Gram-positive pathogens.

METHODS

Bacterial Isolates and Chemicals. A total of 16 clinical isolates of both MRSA and MSSA, *Enterococcus faecalis EF16C51*, *Enterococcus faecium EF16M64*, *Acinetobacter baumannii AB1*, and *Klebsiella pneumonia EPK80* were retrospectively collected between January 1, 2015 and December 31, 2018 at Shenzhen Nanshan People's Hospital, a general tertiary hospital in Shenzhen (Guangdong District, China). The genus and species of the isolates were originally identified and tested for susceptibility to clinically relevant antibiotics by the VITEK 2 compact system (Biomérieux, Marcy l'Etoile, France). Species-appropriate quality control strain *ATCC29213* was used to ensure that the isolates met the standards recommended by Clinical and Laboratory Standards

https://doi.org/10.1021/acsomega.2c06569
ACS Omega 2023, 8, 5415−5425

Institute (CLSI) guidelines. Standard laboratory strains *S. aureus SA113* and *USA300*, *Pseudomonas aeruginosa ATCC27853*, and *Escherichia coli ATCC25922* were kept in our laboratory and used as the representative control. *S. epidermidis 1457* and Δ*vraSR* were kindly given by Qu Di (Shanghai Medical College of Fudan University, Shanghai, China). Procedures involving human participants were carried out in accordance with the ethical standards of Shenzhen Nanshan People's Hospital and the 1964 Helsinki declaration and its subsequently amendments. For this particular study, formal consent was not required. Sertindole, daptomycin (Dap), linezolid (LZD), and vancomycin (VAN) were purchased from MedChemExpress (Shanghai, China).

MIC Test. MICs of sertindole, Dap, LZD, and VAN were determined by the broth microdilution method according to CLSI guidelines (CLSI-M100-S26). Briefly, the suspension density of the overnight bacterial culture solution was adjusted to 0.5 McFarland standard. The bacterial solution was then diluted (1:200) to cation-adjusted Mueller Hinton broth (CAMHB) and added to a 96-well plate with gradient descending concentrations of drug. The condition of MIC assays was determined according to Clinical and Laboratory Standards Institute (CLSI) breakpoints, and the results were observed after 18 h of incubation at 37 °C. The MIC is defined as the lowest concentration of the drug that inhibits the visible growth of planktonic cells.

Time Killing Assay. The time-kill studies of planktonic cells were performed as per our previous study.[37] Briefly, the culture solution of MSSA isolate *YUSA80* and MRSA isolate *YUSA145* in logarithmic phase (OD_{600} = 0.5) was diluted (1:100) respectively with 1× MIC, 2× MIC, and 4× MIC sertindole and incubated on a shaker at 200 rpm. Then, 100 μL of bacterial cultures collected at 0, 2, 6, and 24 h were gradient diluted with tryptone soybean broth (TSB), and 5 μL of aliquots were plated onto tryptone soybean agar (TSA). After being incubated at 37 °C for 24 h, the colonies were counted and assessed by colony-forming units (CFUs).

Growth Curve Analyses. Overnight cultures of MSSA isolate *YUSA80* and MRSA isolate *YUSA145* were sub-cultured (1:1000) in fresh TSB medium and added to the 96-well plate. After sertindole was added to reach the concentrations of 1/8×, 1/4×, 1/2×, and 1× MIC, the plate was placed in the growth curve device (Bioscreen, Piscataway, USA). The optical density at 600 nm (OD_{600}) was read every hour to represent the content of planktonic bacteria in the culture. The incubation temperature is 37 °C.

Biofilm Analysis by Crystal Violet Staining. The crystal violet staining method was used to quantify the forming biofilm of eight representative of MRSA and MSSA isolates (*SA113*, *CHS101*, *YUSA21*, *YUSA80*, *CHS727*, *YUSA145*, *CHS350*, and *YUSA139*). The operation steps for biofilm inhibition are briefly described as follows: Overnight cultures of bacterial solution were diluted 1:1000 by fresh TSBG (tryptic soy broth plus 2% glucose) and placed into a 96-well plate supplied with subinhibitory concentrations of sertindole (1/8×, 1/4×, 1/2×, and 1× MIC). The blank medium without bacterial solution was set as the negative control while the solvent DMSO was added to the final concentration of 0.25% as the positive control. After incubation at 37 °C for 24 h, the supernatant was gently discarded, and wells were washed with sterile PBS three times to remove planktonic cells. After drying at room temperature, adherent biofilms were fixed with 95% methanol and stained with 1% crystal violet (100 μL) for 15 min and washed. Each well was added by 200 μL absolute alcohol and was shaken for 1 min. The optical density at 570 nm (OD_{570}) was then recorded by a micro-plate spectrophotometer to determine the biomass of biofilms. For biofilm disruption, overnight culture of representative *S. aureus* isolates was incubated for 24 h in 96-well cell culture plates to form mature biofilms (without the addition of sertindole). The mature biofilm was rinsed twice with PBS and challenged with sertindole at a series of concentrations and incubated at 37 °C for another 24 h. After incubation, each well was rinsed twice with PBS, and reductions in biofilm biomass (crystal violet staining) and bacterial viability (CFU) were determined.

Detection of Viable Bacteria in Biofilms by a Laser Confocal Microscope. The efficiency of sertindole in *S. aureus* cells embedded in the biofilm was visually assessed by a confocal laser scanning microscope. The overnight culture of MRSA *YUSA145* was 1:200 diluted with fresh TSBG medium and placed into the cell-culture dish (Cornin, United States) and cultured at 37 °C for 24 h to form mature biofilms. After washing with sterile 0.9% NaCl three times, the medium was replaced with fresh TSBG medium containing 4× MIC of sertindole and cultured for another 24 h. Next, after being washed with sterile PBS, Live/Dead dye (Thermo Fisher Scientific, Shanghai, China) was added for a 30-min-dyeing. Then, the biofilm was visualized by a CLSM (OLYMPUS FV3000, Japan).

Morphology Observation by TEM. For observation of the morphology of *S. aureus* cells by TEM, MRSA isolate *YUSA145* were cultured in TSB at 37 °C for 6 h to reach the logarithmic phase. Then, the bacterial cells were collected and treated with 4× MIC of sertindole for another 4 h. After that, cells were washed with phosphate-buffered saline (PBS) and fixed with 2.5% glutaraldehyde at 4 °C for 2 h and 1% osmium for 3 h. The samples were dehydrated in a graded ethanol series and twice in propylene-oxide. Subsequently, the samples were embedded in Epon-Araldite resin for penetration and placed in a model for polymerization. Embedded samples were sectioned with a Reichert Ultracut and then observed under the transmission electron microscope (HT7800, HITACHI, Japan).

Sample Preparation for Quantitative Proteomics. *YUSA145* at exponential growth phase (OD_{600} of 0.5) was added with sertindole to final concentrations that corresponded to 25 μM (1/2× MIC). The sham group was treated with solvent DMSO. Each group was performed with three replicates. The cultures were then incubated at 37 °C for 2 h on a shaker at 200 rpm. After that, the bacteria were harvested by centrifugation at 5000*g* for 10 min at 4 °C. After washing with cold PBS three times, the cell pellets were suspended in RIPA lysis buffer (1% Triton X-100, 1% deoxycholate, 0.1% SDS) with cOmplete protease inhibitor cocktail (catalog No. 05892970001, Roche, Basel, Switzerland). The suspension was then subjected to three rounds of homogenization with glass beads (diameter 0.1 mm) and centrifuged at 12,000*g* for 20 min at 4 °C. Subsequently, the supernatants were collected for protein concentration determination and subsequent quantitative proteomics. Pierce Micro BCA Protein Assay Kit (catalog No. 23227, Thermo Fisher Scientific, MA, USA) was used to determine the protein concentration. One hundred micrograms of extracted protein was reduced with 10 mM DTT (Sigma-Aldrich Co., St. Louis, MO) for 1 h at 70 °C, followed by alkylation using 50 mM iodoacetamide (IAA, Sigma-Aldrich) for 15 min at room temperature in the dark.

https://doi.org/10.1021/acsomega.2c06569
ACS Omega 2023, 8, 5415−5425

The samples were then desalted and buffer-changed three times with 100 μL of 0.5 M ammonium bicarbonate by using Amicon Ultra Centrifugal Filters (10 kDa cutoff; Millipore, Billerica, MA). The proteins were digested with trypsin (Promega, Madison, WI) at a ratio of 1:50 at 37 °C overnight. They were then lyophilized and stored at −80 °C.

Nano LC−MS/MS Analysis. Samples were reconstituted in 0.1% formic acid, among which 10 μg of each sample was injected onto an LC system consisting of an UltiMate 3000 RSLC nanosystem and a C18 precolumn (100 μm × 20 mm, Acclaim PepMap 100 C18, 3 μm), followed by separation using a C18 tip column (75 μm × 250 mm, Acclaim PepMap RSLC, 2 μm). The mobile phases A and B were composed of 0.1% formic acid and 80% acetonitrile in 0.1% formic acid, respectively. The elution system started with 5% B for the first 5 min, followed by a linear gradient from 5% B to 38% B in the following 85 min and from 38% B to 95% B in the next 2 min, sustained at 95% B for another 3 min at a flow rate of 300 nL/min. The column was coupled with a Q Exactive Plus mass spectrometer equipped with the Nano spray ionization (NSI) interface. MS1 scans were acquired over a mass range of 300−1500 m/z with a resolution of 70,000, and the corresponding MS2 spectra were acquired at a resolution of 17,500, collected for maximally 50 ms. All multiply charged ions were used to trigger MS−MS scans, followed by a dynamic exclusion for 30 s. Singly charged precursor ions and ions of undefinable charged states were excluded from fragmentation.

Bioinformatics Analysis for Quantitative Proteomics. The protein identification and quantification were performed using Proteome Discoverer 2.4 base with the Sequest HT against the Uniprot proteome of *Staphylococcus aureus* (Strain: *NCTC 8325/PS 47*). A 2-fold cutoff value was applied to determine upregulated and downregulated proteins in addition to a P-value ≤0.05 in at least two technological replicates. The differentially expressed proteins were uploaded into the OMICSBEAN database (http://www.omicsbean.com) for GO (gene ontology) annotation, including biological process, cellular component, molecular function, and KEGG pathway analysis. The PPI networks were analyzed using the web-based tool STING.

Membrane Permeability and Plasma Membrane Potential Assays. The membrane disruption was identified by SYTOX Green and DiBAC4(3) staining. MRSA isolate *YUSA145* in the exponential growth phase was gathered by centrifugation and adapted to OD_{600} of 0.05 and incubated with 2 μM SYTOX Green and HEPES buffer (5 mM, pH 7.2) at dark. After incubation, the suspension cells were then treated with 1/2× MIC, 1× MIC and 2× MIC sertindole, and solvent 0.1% DMSO and 0.1% Triton were added as control group. The fluorescence intensities were continuously monitored in black polystyrene microtiter plates every 2 min for 20 min by a Cytation 5 cell imaging multimode reader (BioTek, Winooski, VT, USA) at an excitation wavelength of 504 nm and an emission wavelength of 523 nm. For DiBAC4(3) staining, the above suspension logarithmic cells and 2 μM membrane potential-sensitive fluorescent probe DiBAC4(3) were suspended for 5 min. After treatment with different concentrations of sertindole, the fluorescence intensity was monitored at an excitation wavelength of 622 nm and an emission wavelength of 670 nm.

RNA Extract, cDNA Synthesis, and qRT-PCR. *YUSA145* and *S. epidermidis 1457* at exponential growth phase (OD_{600} of 0.5) treated with 25 μM (1/2× MIC) sertindole for 2 h were collected for transcriptional analysis. RNA extraction, cDNA synthesis, and RT-PCR were performed as described previously (Wen et al. 2020). Total bacterial RNA was extracted using the RNeasy Mini kit (Qiagen, Hilden, Germany). CDNA was synthesized with a PrimeScript RT reagent Kit (Takara Bio Inc., Otsu, Japan). Real-time PCR was performed using SYBR Green Perfect mix (Takara Bio, Inc., Otsu, Shiga, Japan) on a QuantStudio 5 (Applied Biosystems, CA, USA) system following the manufacturer's instructions. All sample reactions were performed in triplicate with housekeeping gyrase B subunit gene (*gyrB*) used as an internal standard. All primers used for RT-PCR are listed in Supplementary Table S3.

Statistical Analysis. Graphpad prism 8.0 software was used to process data and draw images. Comparisons of differences in biofilm formation, the transcriptional level, and CFU between the control group and the sertindole-treated group were analyzed using Student's t-test. $P < 0.05$ was considered as statistically significant.

■ ASSOCIATED CONTENT

Supporting Information

The Supporting Information is available free of charge at https://pubs.acs.org/doi/10.1021/acsomega.2c06569.

Inhibitory effect of sertindole on the biofilm formation of *S. aureus* after crystal violet staining (Figure S1); effect of sertindole on the preformed biofilm produced by *S. aureus* (Figure S2); influence of sertindole on the membrane potential of *S. aureus YUSA145* monitored by DiBAC4(3) (Figure S3); sequence alignment of the vraS/vraR two-component system between *S. epidermidis* and *S. aureus* (Figure S4); transcriptional levels of *VraS* and *VraR* in *S. epidermidis 1457* under sertindole stress (Figure S5); MIC values of serindole toward Gram-positive and Gram-negative bacteria (Table S1); MIC values of drugs from indole derivatives against *S. aureus* clinical and standard strains (Table S2); and primers for qRT-PCR in this study (Table S3) (PDF)

■ AUTHOR INFORMATION

Corresponding Authors

Qiwen Deng − *Department of Infectious Diseases and Shenzhen Key Laboratory for Endogenous Infections, Shenzhen Nanshan People's Hospital of Guangdong Medical University, Shenzhen 518052, China*; Email: qiwendeng@hotmail.com

Zhijian Yu − *Department of Infectious Diseases and Shenzhen Key Laboratory for Endogenous Infections, Shenzhen Nanshan People's Hospital of Guangdong Medical University, Shenzhen 518052, China*; Email: yuzhijiansmu@163.com

Zewen Wen − *Department of Infectious Diseases and Shenzhen Key Laboratory for Endogenous Infections, Shenzhen Nanshan People's Hospital of Guangdong Medical University, Shenzhen 518052, China*; orcid.org/0000-0002-9934-2056; Email: wenzw05@163.com

Authors

Yuanyuan Tang − *Department of Infectious Diseases and Shenzhen Key Laboratory for Endogenous Infections, Shenzhen Nanshan People's Hospital of Guangdong Medical University, Shenzhen 518052, China*

https://doi.org/10.1021/acsomega.2c06569
ACS Omega 2023, 8, 5415−5425

Fanlu Zou − *Department of Infectious Diseases and Shenzhen Key Laboratory for Endogenous Infections, Shenzhen Nanshan People's Hospital of Guangdong Medical University, Shenzhen 518052, China*
Chengchun Chen − *Department of Infectious Diseases and Shenzhen Key Laboratory for Endogenous Infections, Shenzhen Nanshan People's Hospital of Guangdong Medical University, Shenzhen 518052, China*
Yiying Zhang − *Department of Infectious Diseases and Shenzhen Key Laboratory for Endogenous Infections, Shenzhen Nanshan People's Hospital of Guangdong Medical University, Shenzhen 518052, China*
Zonglin Shen − *Department of Infectious Diseases and Shenzhen Key Laboratory for Endogenous Infections, Shenzhen Nanshan People's Hospital of Guangdong Medical University, Shenzhen 518052, China*
Yansong Liu − *Department of Infectious Diseases and Shenzhen Key Laboratory for Endogenous Infections, Shenzhen Nanshan People's Hospital of Guangdong Medical University, Shenzhen 518052, China*

Complete contact information is available at: https://pubs.acs.org/10.1021/acsomega.2c06569

Author Contributions

Z.W., Z.Y., and Q.D. conceived and designed the project. Y.T., F.Z., and C.C. performed the biofilm assay and MIC analysis. Y.Z. and Y.L. performed the quantitative proteomics experiment. Z.S. performed the growth curve analysis. All authors participated in data analysis. Z.W. and Y.T. wrote the manuscript with input from all authors. All authors have read and approved the manuscript. All authors participated in data analysis. Y.T., F.Z., and C.C. contributed equally to this work.

Funding

This work was supported by the following grants: National Natural Science Foundation of China (82172283); Natural Science Foundation of Guangdong Province, China (2021A1515011727; 2021A1515110114); Provincial medical funds of Guangdong (A2022497); Shenzhen Key Medical Discipline Construction Fund (SZXK06162); Science, Technology and Innovation Commission of Shenzhen Municipality of basic research funds (JCYJ20190809110622729, JCYJ20190809110209389, JCYJ20190809102219774, and JCYJ20190809151817062), and the Shenzhen Nanshan District Scientific Research Program of the People's Republic of China (NS009, NS117, NS140, NS144, NS066, 2020018, 2020040, and 20200598).

Notes

The authors declare no competing financial interest.
The mass spectrometry proteomics data have been deposited to the ProteomeXchange Consortium (http://proteomecentral.proteomexchange.org) via the iProX partner repository with the dataset identifier PXD035364.

■ ACKNOWLEDGMENTS

The authors would like to thank the reviewer(s) for their valuable comments and suggestions which has greatly improved on the quality of the manuscript. We thank Prof. Di Qu, Dr. Youcong Wu, and Prof. Yang Wu (Fudan University) for providing the *S. epidermidis* VraS/VraR deletion mutant (ΔvraSR).

■ REFERENCES

(1) Turner, N. A.; Sharma-Kuinkel, B. K.; Maskarinec, S. A.; Eichenberger, E. M.; Shah, P. P.; Carugati, M.; Holland, T. L.; Fowler, V. G. Methicillin-resistant Staphylococcus aureus: an overview of basic and clinical research. *Nat. Rev. Microbiol.* **2019**, *17*, 203−218.
(2) Calfee, D. P. Trends in Community Versus Health Care-Acquired Methicillin-Resistant Staphylococcus aureus Infections. *Curr. Infect. Dis. Rep.* **2017**, *19*, 48.
(3) Juhas, M. Horizontal gene transfer in human pathogens. *Crit. Rev. Microbiol.* **2015**, *41*, 101−108.
(4) Tacconelli, E.; Carrara, E.; Savoldi, A.; Harbarth, S.; Mendelson, M.; Monnet, D. L.; Pulcini, C.; Kahlmeter, G.; Kluytmans, J.; Carmeli, Y.; Ouellette, M.; Outterson, K.; Patel, J.; Cavaleri, M.; Cox, E. M.; Houchens, C. R.; Grayson, M. L.; Hansen, P.; Singh, N.; Theuretzbacher, U.; Magrini, N.; Aboderin, A. O.; al-Abri, S. S.; Awang Jalil, N.; Benzonana, N.; Bhattacharya, S.; Brink, A. J.; Burkert, F. R.; Cars, O.; Cornaglia, G.; Dyar, O. J.; Friedrich, A. W.; Gales, A. C.; Gandra, S.; Giske, C. G.; Goff, D. A.; Goossens, H.; Gottlieb, T.; Guzman Blanco, M.; Hryniewicz, W.; Kattula, D.; Jinks, T.; Kanj, S. S.; Kerr, L.; Kieny, M. P.; Kim, Y. S.; Kozlov, R. S.; Labarca, J.; Laxminarayan, R.; Leder, K.; Leibovici, L.; Levy-Hara, G.; Littman, J.; Malhotra-Kumar, S.; Manchanda, V.; Moja, L.; Ndoye, B.; Pan, A.; Paterson, D. L.; Paul, M.; Qiu, H.; Ramon-Pardo, P.; Rodríguez-Baño, J.; Sanguinetti, M.; Sengupta, S.; Sharland, M.; Si-Mehand, M.; Silver, L. L.; Song, W.; Steinbakk, M.; Thomsen, J.; Thwaites, G. E.; van der Meer, J. W. M.; van Kinh, N.; Vega, S.; Villegas, M. V.; Wechsler-Fördös, A.; Wertheim, H. F. L.; Wesangula, E.; Woodford, N.; Yilmaz, F. O.; Zorzet, A. Discovery, research, and development of new antibiotics: the WHO priority list of antibiotic-resistant bacteria and tuberculosis. *Lancet Infect. Dis.* **2018**, *18*, 318−327.
(5) Ippolito, G.; Leone, S.; Lauria, F. N.; Nicastri, E.; Wenzel, R. P. Methicillin-resistant Staphylococcus aureus: the superbug. *Int. J. Infect. Dis.* **2010**, *14*, S7−S11.
(6) Kourtis, A. P.; Hatfield, K.; Baggs, J.; Mu, Y.; See, I.; Epson, E.; Nadle, J.; Kainer, M. A.; Dumyati, G.; Petit, S.; Ray, S. M.; Ham, D.; Capers, C.; Ewing, H.; Coffin, N.; McDonald, L. C.; Jernigan, J.; Cardo, D. Vital Signs: Epidemiology and Recent Trends in Methicillin-Resistant and in Methicillin-Susceptible Staphylococcus aureus Bloodstream Infections - United States. *Morb. Mortal. Wkly. Rep.* **2019**, *68*, 214−219.
(7) Hall, C. W.; Mah, T. F. Molecular mechanisms of biofilm-based antibiotic resistance and tolerance in pathogenic bacteria. *FEMS Microbiol. Rev.* **2017**, *41*, 276−301.
(8) Parsek, M. R.; Singh, P. K. Bacterial biofilms: an emerging link to disease pathogenesis. *Annu. Rev. Microbiol.* **2003**, *57*, 677−701.
(9) Mohammed, Y. H. E.; Manukumar, H. M.; Rakesh, K. P.; Karthik, C. S.; Mallu, P.; Qin, H. L. Vision for medicine: Staphylococcus aureus biofilm war and unlocking key's for anti-biofilm drug development. *Microb. Pathog.* **2018**, *123*, 339−347.
(10) Suresh, M. K.; Biswas, R.; Biswas, L. An update on recent developments in the prevention and treatment of Staphylococcus aureus biofilms. *Int. J. Med. Microbiol.* **2019**, *309*, 1−12.
(11) Corsello, S. M.; Bittker, J. A.; Liu, Z.; Gould, J.; McCarren, P.; Hirschman, J. E.; Johnston, S. E.; Vrcic, A.; Wong, B.; Khan, M.; Asiedu, J.; Narayan, R.; Mader, C. C.; Subramanian, A.; Golub, T. R. The Drug Repurposing Hub: a next-generation drug library and information resource. *Nat. Med.* **2017**, *23*, 405−408.
(12) Miró-Canturri, A.; Ayerbe-Algaba, R.; Smani, Y. Drug Repurposing for the Treatment of Bacterial and Fungal Infections. *Front. Microbiol.* **2019**, *10*, 41.
(13) Leucht, S.; Cipriani, A.; Spineli, L.; Mavridis, D.; Orey, D.; Richter, F.; Samara, M.; Barbui, C.; Engel, R. R.; Geddes, J. R.; Kissling, W.; Stapf, M. P.; Lässig, B.; Salanti, G.; Davis, J. M. Comparative efficacy and tolerability of 15 antipsychotic drugs in schizophrenia: a multiple-treatments meta-analysis. *Lancet* **2013**, *382*, 951−962.
(14) Huggins, W. M.; Barker, W. T.; Baker, J. T.; Hahn, N. A.; Melander, R. J.; Melander, C. Meridianin D Analogues Display

Antibiofilm Activity against MRSA and Increase Colistin Efficacy in Gram-Negative Bacteria. *ACS Med. Chem. Lett.* **2018**, *9*, 702−707.
(15) Dennis, G., Jr.; Sherman, B. T.; Hosack, D. A.; Yang, J.; Gao, W.; Lane, H. C.; Lempicki, R. A. DAVID: Database for Annotation, Visualization, and Integrated Discovery. *Genome Biol.* **2003**, *4*, P3.
(16) Percy, M. G.; Gründling, A. Lipoteichoic acid synthesis and function in gram-positive bacteria. *Annu. Rev. Microbiol.* **2014**, *68*, 81−100.
(17) Ghebremedhin, B.; Layer, F.; König, W.; König, B. Genetic classification and distinguishing of Staphylococcus species based on different partial gap, 16S rRNA, hsp60, rpoB, sodA, and tuf gene sequences. *J. Clin. Microbiol.* **2008**, *46*, 1019−1025.
(18) Becker, K.; Heilmann, C.; Peters, G. Coagulase-negative staphylococci. *Clin. Microbiol. Rev.* **2014**, *27*, 870−926.
(19) Du, X.; Larsen, J.; Li, M.; Walter, A.; Slavetinsky, C.; Both, A.; Sanchez Carballo, P. M.; Stegger, M.; Lehmann, E.; Liu, Y.; Liu, J.; Slavetinsky, J.; Duda, K. A.; Krismer, B.; Heilbronner, S.; Weidenmaier, C.; Mayer, C.; Rohde, H.; Winstel, V.; Peschel, A. Staphylococcus epidermidis clones express Staphylococcus aureus-type wall teichoic acid to shift from a commensal to pathogen lifestyle. *Nat. Microbiol.* **2021**, *6*, 757−768.
(20) Wu, Y.; Meng, Y.; Qian, L.; Ding, B.; Han, H.; Chen, H.; Bai, L.; Qu, D.; Wu, Y. The Vancomycin Resistance-Associated Regulatory System VraSR Modulates Biofilm Formation of Staphylococcus epidermidis in an ica-Dependent Manner. *mSphere* **2021**, *6*, No. e0064121.
(21) Nosengo, N. Can you teach old drugs new tricks? *Nature* **2016**, *534*, 314−316.
(22) Sánchez, C.; Arnt, J.; Dragsted, N.; Hyttel, J.; Lembøl, H. L.; Meier, E.; Perregaard, J.; Skarsfeldt, T. Neurochemical and in vivo pharmacological profile of sertindole, a limbic-selective neuroleptic compound. *Drug Develop. Res.* **1991**, *22*, 239−250.
(23) Hyttel, J.; Nielsen, J. B.; Nowak, G. The acute effect of sertindole on brain 5-HT2, D2 and alpha 1 receptors (ex vivo radioreceptor binding studies). *J. Neural Transm.* **1992**, *89*, 61−69.
(24) Yoon, Y. S.; Jang, Y.; Hoenen, T.; Shin, H.; Lee, Y.; Kim, M. Antiviral activity of sertindole, raloxifene and ibutamoren against transcription and replication-competent Ebola virus-like particles. *BMB Rep.* **2020**, *53*, 166−171.
(25) Shin, J. H.; Park, S. J.; Kim, E. S.; Jo, Y. K.; Hong, J.; Cho, D. H. Sertindole, a potent antagonist at dopamine D_2 receptors, induces autophagy by increasing reactive oxygen species in SH-SY5Y neuroblastoma cells. *Biol. Pharm. Bull.* **2012**, *35*, 1069−1075.
(26) Zhang, W.; Zhang, C.; Liu, F.; Mao, Y.; Xu, W.; Fan, T.; Sun, Q.; He, S.; Chen, Y.; Guo, W.; Tan, Y.; Jiang, Y. Antiproliferative activities of the second-generation antipsychotic drug sertindole against breast cancers with a potential application for treatment of breast-to-brain metastases. *Sci. Rep.* **2018**, *8*, 15753.
(27) Schilcher, K.; Horswill, A. R. Staphylococcal Biofilm Development: Structure, Regulation, and Treatment Strategies. *Microbiol. Mol. Biol. Rev.* **2020**, *84*, No. e00026-19.
(28) Van Acker, H.; Coenye, T. The Role of Reactive Oxygen Species in Antibiotic-Mediated Killing of Bacteria. *Trends Microbiol.* **2017**, *25*, 456−466.
(29) Chen, F. J.; Lauderdale, T. L.; Lee, C. H.; Hsu, Y. C.; Huang, I. W.; Hsu, P. C.; Yang, C. S. Effect of a Point Mutation in mprF on Susceptibility to Daptomycin, Vancomycin, and Oxacillin in an MRSA Clinical Strain. *Front. Microbiol.* **2018**, *9*, 1086.
(30) Ernst, C. M.; Slavetinsky, C. J.; Kuhn, S.; Hauser, J. N.; Nega, M.; Mishra, N. N.; Gekeler, C.; Bayer, A. S.; Peschel, A. Gain-of-Function Mutations in the Phospholipid Flippase MprF Confer Specific Daptomycin Resistance. *MBio* **2018**, *9*, No. e01659-18.
(31) Ernst, C. M.; Peschel, A. MprF-mediated daptomycin resistance. *Int. J. Med. Microbiol.* **2019**, *309*, 359−363.
(32) Thitiananpakorn, K.; Aiba, Y.; Tan, X. E.; Watanabe, S.; Kiga, K.; Sato'o, Y.; Boonsiri, T.; Li, F. Y.; Sasahara, T.; Taki, Y.; Azam, A. H.; Zhang, Y.; Cui, L. Association of mprF mutations with cross-resistance to daptomycin and vancomycin in methicillin-resistant Staphylococcus aureus (MRSA). *Sci. Rep.* **2020**, *10*, 16107.
(33) Jiang, S.; Zhuang, H.; Zhu, F.; Wei, X.; Zhang, J.; Sun, L.; Ji, S.; Wang, H.; Wu, D.; Zhao, F.; Yan, R.; Yu, Y.; Chen, Y. The Role of mprF Mutations in Seesaw Effect of Daptomycin-Resistant Methicillin-Resistant Staphylococcus aureus Isolates. *Antimicrob. Agents Chemother.* **2022**, *66*, No. e0129521.
(34) Kuroda, M.; Kuroda, H.; Oshima, T.; Takeuchi, F.; Mori, H.; Hiramatsu, K. Two-component system VraSR positively modulates the regulation of cell-wall biosynthesis pathway in Staphylococcus aureus. *Mol. Microbiol.* **2003**, *49*, 807−821.
(35) Hafer, C.; Lin, Y.; Kornblum, J.; Lowy, F. D.; Uhlemann, A. C. Contribution of selected gene mutations to resistance in clinical isolates of vancomycin-intermediate Staphylococcus aureus. *Antimicrob. Agents Chemother.* **2012**, *56*, 5845−5851.
(36) Tajbakhsh, G.; Golemi-Kotra, D. The dimerization interface in VraR is essential for induction of the cell wall stress response in Staphylococcus aureus: a potential druggable target. *BMC Microbiol.* **2019**, *19*, 153.
(37) Zhang, Y.; Zhang, Y.; Chen, C.; Cheng, H.; Deng, X.; Li, D.; Bai, B.; Yu, Z.; Deng, Q.; Guo, J.; Wen, Z. Antibacterial activities and action mode of anti-hyperlipidemic lomitapide against Staphylococcus aureus. *BMC Microbiol.* **2022**, *22*, 114.

https://doi.org/10.1021/acsomega.2c06569
ACS Omega 2023, 8, 5415−5425